

Photopolymer-Based Diffractive and MMI Waveguide Couplers

Anthony V. Mule', Ricardo Villalaz, Thomas K. Gaylord, and James D. Meindl

Abstract—Diffractive and multimode-interference waveguide couplers constructed from photopolymer materials are presented. Two-material grating-in-the-waveguide optical interconnects are fabricated and tested with respect to waveguide propagation loss and grating out-coupling. Waveguide/grating interconnects have been constructed with both index-defined and air-clad waveguide channel regions, where air-clad channels exhibit measured propagation losses of $\alpha_{wg} = 0.47 - 3$ dB/cm. Measurements of output coupling coefficients of volume grating couplers terminating various waveguide channels range from $\alpha_g = 1.4 - 5.3$ mm⁻¹. A 1×4 photopolymer-based multimode-interference power-splitting coupler fabricated and tested for the provision of in-plane optical coupling is found to demonstrate 0.3–0.6-dB output power uniformity.

Index Terms—Holographic gratings, optical coupling, optical interconnections, optical planar waveguide couplers, waveguides.

I. INTRODUCTION

OPTICAL waveguides integrated onto printed wiring boards and within chip-scale packages require efficient means of both out-of-plane signal coupling (e.g., into and out of interconnect channels) and in-plane signal coupling (e.g., between fanout paths). With respect to out-of-plane signal coupling, volume diffraction grating couplers are capable of high-efficiency input (e.g., 80% [1]) and output (e.g., 95% [2]) coupling. The availability of photopolymer materials suitable for constructing such high-performance couplers, however, is limited. For example, the photopolymer reported in [1] and [2] (Omnidex HRF 600 from Dupont) is capable of submicron resolution, low shrinkage, low moisture absorption, and high index modulation for high-performance grating formation. Although optimized for holographic gratings, this material is not intended for use as a waveguide material, as reflected, for example, through the intrinsic material absorption loss and need for plasma-definition of waveguide channels. With respect to in-plane signal coupling, multimode interference (MMI) power-splitting couplers offer fanouts greater than two, compact dimensions, and high tolerance to polarization variations, for example. In addition, the ability to route optical signals with high uniformity between fanout paths reduces timing uncertainties due to variations in received power.

Avatrel photopolymer (from Promerus, LLC) is an epoxy-based polynorbornene. This polymer exhibits several properties advantageous to wafer-level packaging, including

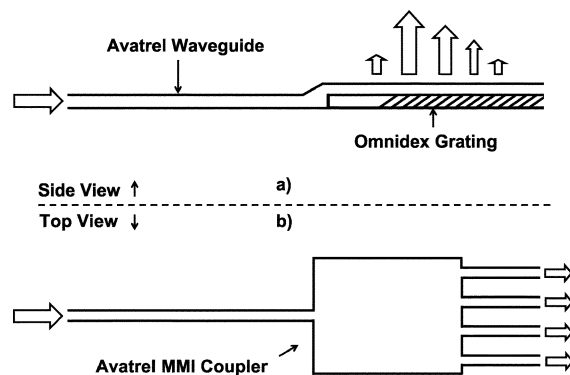


Fig. 1. Optical waveguide coupler structures. (a) Two-material waveguide/grating interconnect with out-of-plane diffractive coupler. (b) In-plane MMI coupler.

low dielectric constant, low moisture absorption, and low modulus. This letter reports, to our knowledge, the first fabrication and testing of two-material grating coupler-in-the-waveguide optical interconnects for out-of-plane coupling, where waveguide and grating regions are constructed from *separate* photopolymer materials. The small refractive index contrast Δn ($\Delta n = 9 \times 10^{-3}$) between and similar processing conditions associated with Avatrel and Omnidex photopolymer materials allows for the construction of Avatrel/Omnidex waveguide/grating coupler interconnects with no detectable reflection loss at the material interface. In addition, the fabrication and testing of MMI power-splitting couplers from Avatrel photopolymer material for in-plane coupling are demonstrated for the first time. Adjustment of the photopolymer viscosity through solvent addition allows for the creation of compact equal-power MMI power-splitting couplers with $2/6$ - μ m width/pitch fanout waveguides. Both out-of-plane diffractive grating couplers and in-plane MMI couplers are depicted in Fig. 1.

II. TWO-MATERIAL WAVEGUIDE/GRATING DIFFRACTIVE COUPLERS

The construction of two-material interconnects begins with the fabrication of slab (~ 10 – 12 mm wide) gratings consisting of a 6 - μ m-thick Omnidex film atop a transparent fused silica substrate [2]. A nonfocusing, preferential-order volume grating with period $\Lambda = 0.3$ μ m and slant angle $\Phi = 45^\circ$ is written in the laminate Omnidex film through a two-beam interferometric exposure. The grating profile, defined through monomer/polymer diffusion, is fixed prior to film cure with an additional 150 mJ/cm² uniform one-beam exposure. The substrate is then heated on a 150 °C hotplate, after which the remaining Mylar film encasing the Omnidex film is removed.

Manuscript received March 31, 2004; revised July 12, 2004. This work was supported by the Semiconductor Research Corporation (SRC) and by the Microelectronics Advanced Research Corporation (MARCO).

The authors are with the Microelectronics Research Center, Georgia Institute of Technology, Atlanta, GA 30332-0269 USA (e-mail: tvmule@ieee.org).

Digital Object Identifier 10.1109/LPT.2004.835193

The sample is cured at 150 °C, and each slab unpatterned substrate is tested following cure to obtain the Bragg angle and the input coupling efficiency prior to patterning.

Raised-strip grating channels are produced from the slab film through hard-mask patterning and reactive ion etching. A 0.5- μm Au film is sputtered onto the sample using a dc sputter, and is patterned using Shipley 1813 photoresist into 100- μm -wide channels. A 30-s 300-W/300-mT/50-sccm O_2 plasma descum removes any residual photoresist prior to Au mask etch. Wet etching of the Au mask is performed using a custom Au etchant consisting of 40 g potassium iodide (KI), 10-g iodine (I_2), and 400 mL of DI water. Since Omnidex photopolymer is harmed by wet chemicals used to remove photoresist (e.g., Acetone), the resist is instead removed during reactive ion etching of the Omnidex film. A 300-W 50-mT 50-sccm O_2 plasma is created to etch the Omnidex film and the hard-mask photoresist. Plasma etching of cured Omnidex films results typically in the presence of a ~ 200 Å residual film which must be removed prior to waveguide formation. Removal of this film is achieved by undercutting the film with a short buffered oxide etch.

Once the grating channels have been defined, the construction of either index-defined or raised-strip air-clad waveguide channels leading into each diffraction grating can proceed. Both technologies involve spin-application, soft bake, photodefinition, postexposure bake, and cure of a 6.5- μm -thick film of Avatrel photopolymer. The key differences between index-defined/air-clad waveguide technologies is 1) the absence/presence of a 120-nm glass passivation layer atop grating channels prior to Avatrel deposition, 2) the use of a positive-tone/negative-tone photomask during photodefinition, and 3) the absence/presence of a wet-development step, respectively. In the case of air-clad channels, the passivation layer was found to promote adhesion between Avatrel and Omnidex photopolymers in the presence of a spray development. The deposition temperature of the passivation layer matches the cure temperature of the Omnidex photopolymer, thereby avoiding grating degradation associated with higher temperature deposition. Spray-development of air-clad channels following photodefinition is achieved using Avatrel 1000 developer. Samples are rinsed in isopropyl alcohol, spun dry, and placed in an N_2 -purged oven. Curing of all Avatrel films takes place using a ramped cure schedule, where the film is raised from room temperature to 160 °C at 3.2°/min, held for 1 h, reduced to 150 °C at 2°/min, held for 10 min, and then reduced to room temperature at 3.2 °C/min. A top-down micrograph of air-clad Avatrel/Omnidex waveguide/grating channels is shown in Fig. 2. Rotation stage measurements of Bragg angle and input coupling efficiency taken before and after channel formation are depicted in Fig. 3. No shift in the angular location of the input-coupling peaks due to grating patterning or waveguide processing are observed relative to measurements taken before patterning, indicating the high fidelity of the fabrication process.

Grating coupling coefficients and waveguide propagation loss metrics for air-clad and index-defined channels are collected using the image capture method. A charged-coupled device camera collects a bitmap image of photons diffracted/scattered from grating/waveguide regions, where the exposure time used to collect data is such that the brightness value

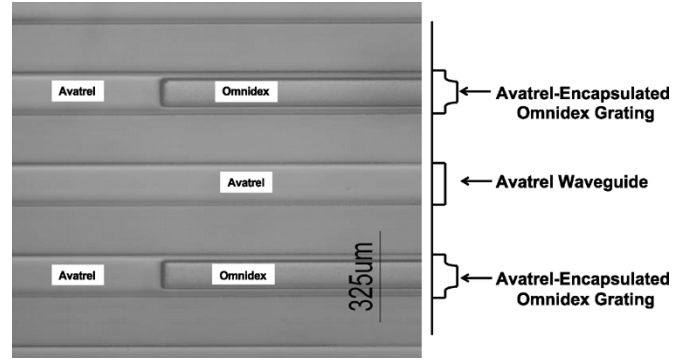


Fig. 2. Top-down micrograph of air-clad Avatrel/Omnidex waveguide/grating optical interconnect channels.

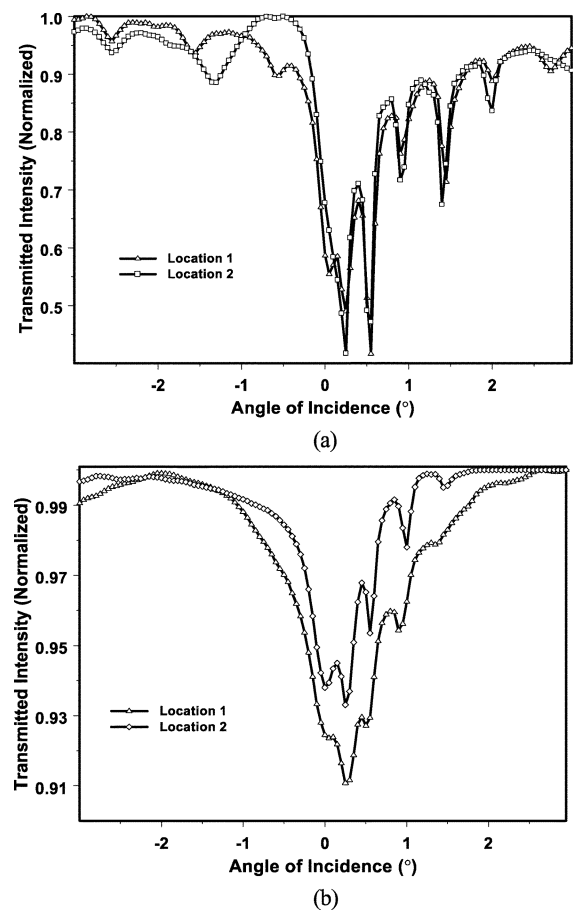


Fig. 3. Bragg angle input coupling efficiency measurements of volume grating coupler (a) before and (b) after patterning. Each measurement location refers to a unique position of a collimated HeNe test beam on the substrate during rotation stage measurements. In the case of postpatterning measurements, the test beam falls onto a finite number of channels such that $\sim 3\%$ beam overlap is achieved with grating regions.

of individual pixels fall just below saturation. The bitmap is loaded into Matlab and fit to an exponential using a robust bisquare linear least-squares fit algorithm. Using this method, the propagation loss coefficient α_{wg} ranges from $\alpha_{wg} = 0.47$ to 3.09 dB/cm, while the coupling coefficient α_g ranges from 1.56 to 5.3 mm^{-1} for fabricated air-clad channels. Fig. 4 illustrates an example of the robust linear least squares fit observed for

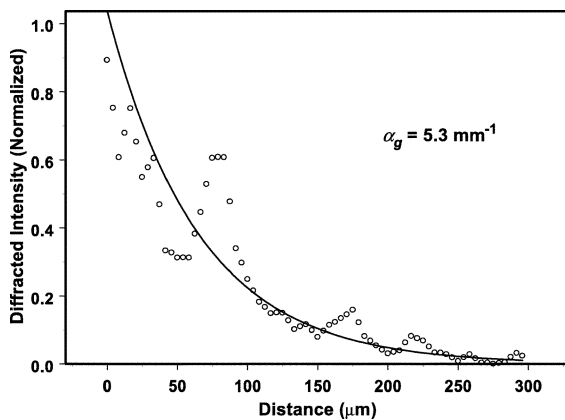


Fig. 4. Robust linear least squares fit (solid line) to diffracted intensity of patterned grating channel indicating a coupling coefficient of $\alpha_g = 5.3 \text{ mm}^{-1}$.

grating-diffracted power. Similar measurements corresponding to index-defined waveguides indicate propagation losses of $\alpha_{\text{wg}} = 5.4 - 8.8 \text{ dB/cm}$.

III. MMI POWER-SPLITTING COUPLER

In addition to interconnect structures providing out-of-plane optical signal coupling, Avatrel-based power-splitting couplers have also been fabricated to facilitate in-plane signal coupling between lateral fanout paths. In its simplest form, an MMI device consists of a single-mode waveguide center-feeding a wide multimode rectangular cavity whose dimensions are dictated by the desired fanout. MMI power-splitting couplers demonstrate high tolerance to polarization and wavelength variations, and can operate with excess power splitting losses $< 1 \text{ dB}$ and output power uniformities between $0.3\text{--}0.9 \text{ dB}$ [3]–[5]. In addition, a key advantage of MMI power-splitting couplers is the ability to fabricate devices with fanouts greater than two. For example, a 1×32 sol-gel MMI device is reported in [6] that demonstrates an excess loss of less than 0.75 dB and an output power uniformity of 0.95 dB .

Avatrel MMI splitters with $2\text{-}\mu\text{m}$ -wide output waveguides and $4\text{--}6\text{-}\mu\text{m}$ pitch have been fabricated using the same process conditions developed for air-clad waveguide/grating interconnects. Fig. 5 illustrates optical profilometer measurements of such devices following film development and before the final cure step. Measurement of power uniformity between output channel waveguides of fully fabricated devices is performed by exciting the device and capturing an unsaturated image of the output waveguides. A pixel matrix centered about the maximum-count pixel of each waveguide is specified and all pixels within the matrix are summed. In this manner, the output power uniformity of a 1×4 device with $3/7\text{-}\mu\text{m}$ width/pitch output waveguides has been found to be $0.3\text{--}0.6 \text{ dB}$. Fig. 6 illustrates a contour plot of the image captured for this device, illustrating a high degree of uniformity between fanout waveguides.

IV. CONCLUSION

Diffractive and multimode-interference couplers constructed from photopolymer materials are presented for out-of-plane and in-plane coupling, respectively. The investigation and realization of two-material volume grating-in-the-waveguide optical interconnects represents a solution to the limited availability

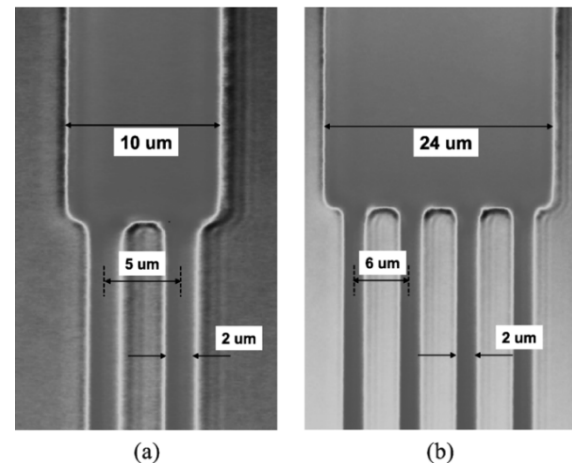


Fig. 5. Optical profilometer measurements of MMI power-splitting couplers fabricated using Avatrel photopolymer. (a) 1×2 device with $2/5\text{-}\mu\text{m}$ width/pitch output waveguides. (b) 1×4 device with $2/6\text{-}\mu\text{m}$ width/pitch output waveguides. Each image is captured at a unique magnification.

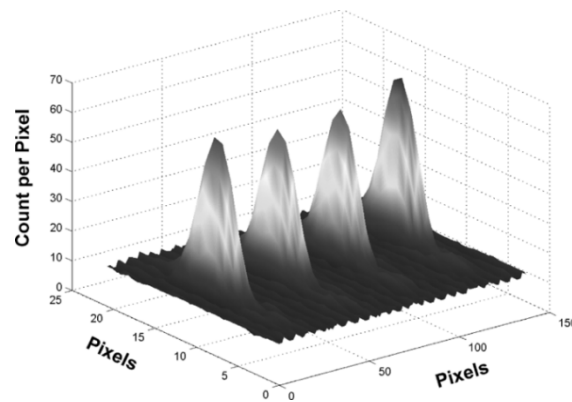


Fig. 6. Contour plot of measured relative intensity between power splitter output waveguides. A relative power uniformity of $0.3\text{--}0.6 \text{ dB}$ is recorded for this device.

of photopolymer materials optimized for both low propagation loss waveguides and high-coupling-coefficient diffraction gratings. Air-clad waveguides exhibiting propagation losses as low as $\alpha_{\text{wg}} = 0.47 \text{ dB/cm}$ and gratings exhibiting coupling coefficients as high as $\alpha_g = 5.3 \text{ mm}^{-1}$ are demonstrated. In addition, a 1×4 MMI power-splitting coupler constructed from Avatrel photopolymer for in-plane coupling exhibits $0.3\text{--}0.6\text{-dB}$ output power uniformity.

REFERENCES

- [1] S. M. Schultz, "High-efficiency volume grating coupler," Ph.D. dissertation, Georgia Inst. of Technology, 1999.
- [2] S. M. Schultz, E. N. Glytsis, and T. K. Gaylord, "Volume grating preferential-order focusing waveguide coupler," *Opt. Lett.*, vol. 24, pp. 1708–1710, Dec. 1999.
- [3] L. B. Soldano and E. C. M. Pennings, "Optical multimode interference devices based on self-imaging: Principles and applications," *J. Light-wave Technol.*, vol. 13, pp. 615–627, Apr. 1995.
- [4] O. Bryngdahl, "Image formation using self-imaging techniques," *J. Opt. Soc. Amer.*, vol. 63, pp. 416–419, 1973.
- [5] E. C. M. Pennings, R. J. Deri, R. Bhat, T. R. Hayes, and N. C. Andreadakis, "Ultracompact, all-passive optical 90° -hybrid on InP using self-imaging," *IEEE Photon. Technol. Lett.*, vol. 5, pp. 701–703, June 1993.
- [6] M. A. Fardad and M. Fallahi, "Sol-gel multimode interference power splitters," *IEEE Photon. Technol. Lett.*, vol. 11, pp. 697–699, June 1999.